Neutron scattering from the Heisenberg ferromagnets EuO and EuS. I. The exchange interactions*

L. Passell
Brookhaven National Laboratory, Upton, New York 11973

O. W. Dietrich† and J. Als-Nielsen†
Research Establishment Risø, 4000 Roskilde, Denmark

(Received 13 May 1976)

Inelastic-neutron-scattering methods have been used to measure the spin-wave spectrum in EuO and EuS over the entire Brillouin zone. The samples were polycrystalline powders enriched in ^{153}Eu. Defining the interaction between pairs of spins to be $-2J_{nm}\vec{S}_n\cdot\vec{S}_m$, we obtained for EuO, $J_1/k_B = 0.606 \pm 0.008$°K and $J_2/k_B = 0.119 \pm 0.015$°K; for EuS, $J_1/k_B = 0.236 \pm 0.009$°K and $J_2/k_B = -0.118 \pm 0.011$°K. The measured Curie temperatures for EuO, 69.15 ± 0.05°K, and for EuS, 16.57 ± 0.01°K, are in excellent agreement with calculated values obtained from series expansions relating T_C to the exchange constants. In EuO, the neutron scattering measurements determine J_1 and J_2 separately. Although separate values for the exchange constants were reported in earlier experiments, we show that in fact only the spin-wave stiffness constant of EuO, which is proportional to $J_1 + J_2$, was actually determined. In EuS, our values of J_1 and J_2 agree with a reanalysis of the specific-heat data.

I. INTRODUCTION

One of the more remarkable achievements of contemporary solid-state physics has been the replacement of the classical thermodynamic approach to magnetism in solids by microscopic theories in which magnetic behavior is related to the underlying interactions between atoms. Current theories are capable of describing the properties of some of the simpler magnetic systems in considerable detail. Among such systems, the most completely explored theoretically is probably the isotropic exchange-coupled magnet with localized moments, i.e., the simple isotropic Heisenberg magnet.

It is fortunate that there exist in nature materials which are very good representations of such systems. Prominent among these are the divalent europium chalcogenides, a series of magnetic insulators in which the magnetic Eu^{2+} ions (in spherically symmetric $^8S_{7/2}$ spin states) form simple fcc lattices. Two of the compounds in this series, EuO and EuS, are ferromagnets[1,2]; a third, EuSe, exhibits both an antiferromagnetically ordered phase and a two-component ferrimagnetic and antiferromagnetic phase,[3] while the last, EuTe, is an antiferromagnet.[4] All members of the series are of interest, but EuO and EuS are of particular importance because they are the only known examples of simple Heisenberg *ferromagnets*.

Since the theory of these particular systems has been developed to a relatively advanced state, there are many quantitative comparisons which can be made with experiments. Thus it is not surprising that both EuO and EuS have been widely studied by all of the traditional methods used for magnetic investigations and that their macroscopic thermodynamic properties are relatively well documented.[5-12] But until recently, aside from what could be inferred from macroscopic results, little was known about their microscopic properties, although these are actually of more basic concern to the theory. This unusual state of affairs resulted primarily from the fact that europium is a strong neutron absorber. Thus inelastic-neutron-scattering data, normally the best source of microscopic information for magnetic systems, have not been available for europium compounds.

Although absorption makes neutron scattering experiments difficult, it does not necessarily rule them out altogether. We therefore began some years ago to consider the feasibility of making inelastic scattering studies of EuO and EuS. Ultimately, we concluded that the best approach was the direct and obvious one: a thin-slab sample geometry with the absorption reduced as much as possible by using materials prepared with separated ^{153}Eu (which has the smaller absorption cross section of the two naturally occurring isotopes). While not without its limitations, this technique proved to be surprisingly successful in practice. Using it we were able to study the microscopic magnetic properties of both EuO and EuS in considerable detail. This included investigations of the static critical properties of both compounds, of the behavior of their spin waves at low temperatures, and, in EuO, of spin waves at temperatures approaching the Curie temperature T_C. These experiments have all been briefly described in the literature.[13-15]

It is our intention in this and the two following papers to present a comprehensive account of all of our measurements, and where relevant, to

make detailed comparisons with other experiments and with theory. Also included will be the results of further neutron scattering studies of EuO which have not as yet been reported. These are of two kinds. First, we have extended our investigations of spin dynamics to cover the region from low temperatures to about $2T_C$ and second, we have made measurements of the scattered intensity below T_C at very small values of the wave-vector transfer κ.

This paper (hereafter referred to as I) will be concerned with the determination of the exchange interactions in EuO and EuS by direct measurement of the spin-wave spectra. Paper II will contain the details of our observations of static critical phenomena in both compounds. In paper III we will review our investigations of spin dynamics in EuO. Each paper is intended to be reasonably self-contained so that the basic results of one can be understood without the need for excessive reference to the others.

II. EXCHANGE INTERACTIONS IN THE EUROPIUM CHALCOGENIDES AND METHODS OF DETERMINING THE EXCHANGE CONSTANTS

Although a considerable effort has been devoted to identifying exchange mechanisms in nonmetallic $3d$ compounds, relatively little has been done as yet with the equivalent rare-earth $4f$ insulators. Kasuya[16] has made the most complete analysis of possible exchange mechanisms in the europium chalcogenides. Briefly, his picture of exchange in these compounds is as follows:

Since the $4f$ electrons are highly localized, the exchange coupling between Eu^{2+} ions occurs not via direct overlap of $4f$ states but by indirect and superexchange mechanisms. The main point, according to Kasuya, is that the $5d$ wave functions are more extended than the $4f$ and overlap sufficiently to form an unoccupied conduction band. Exchange between nearest-neighbor (nn) Eu^{2+} cations therefore proceeds mainly by means of an indirect process in which a $4f$ electron is transferred to a vacant $5d$ state, couples ferromagnetically via d-f exchange to the $4f$ spin at the nn Eu site, and then returns to its initial $4f$ state.

The next-nearest-neighbor (nnn) interaction is thought to involve several mechanisms. One is a superexchange process in which the p states of the anion connect nnn cations. In this case Kasuya suggests that anion p electrons are transferred to $5d$ states of neighboring Eu^{2+} cations forming 180° bonds and thus coupling the $4f$ spins antiferromagnetically through d-f echange interactions. There is also a competing process, the Kramers-Anderson mechanism, involving transfer of a $4f$ electron to a nnn $4f$ state. This then forms a pair of ions, Eu^{3+} and Eu^{+}. Of itself, the Kramers-Anderson mechanism does not contribute significantly to the nnn exchange in the europium chalcogenides. However, the cross term between this process and the d-f exchange does appear to contribute and, because it is of opposite sign to the d-f exchange, has an important influence on magnetic behavior.

Both nn and nnn exchange mechanisms are very sensitive to the interionic distance. As the distance decreases, the nn ferromagnetic exchange increases rapidly. This is also the case with the cross term between the Kramers-Anderson mechanism and d-f exchange. Superexchange via anion p electrons, which dominates the nnn exchange at large distances, is apparently less sensitive to interionic distance. Hence, as the distance between ions decreases, the cross term becomes relatively more important. Ultimately, at small interionic distances Kasuya suggests that the cross term becomes dominant and the nnn exchange then becomes ferromagnetic. As we will show, this behavior is consistent with the experimental evidence.

In this brief outline we have only mentioned what are thought to be the most important exchange mechanisms. We suggest that those interested in more detail consult Kasuya's paper, which also contains references to related work in this field.

Let us now review, also briefly, the methods by which exchange interactions are investigated experimentally. In the system we are considering, the interaction between two localized spins $\vec{S}_n$ and $\vec{S}_m$ at lattice points $\vec{R}_n$ and $\vec{R}_m$ is assumed to be of the Heisenberg type, i.e., the interaction energy is expressed in terms of an exchange constant J_{nm}, and is of the form

$$-2J_{nm}\vec{S}_n\cdot\vec{S}_m. \tag{1}$$

The values of the exchange constants can be determined in a variety of ways, including nuclear-magnetic-resonance (NMR),[7,8] ferromagnetic- (and antiferromagnetic-) spin-resonance,[11] specific-heat,[5,6] and inelastic-neutron-scattering measurements.[14] NMR and spin resonance measure, respectively, the local field at the nucleus and the average field experienced by the $4f$ spins. In both cases the field is assumed to be proportional to the magnetization which is related to the thermally populated part of the spin-wave spectrum. In turn, the spin-wave population is determined by the values of the exchange constants. The magnetic contribution to the specific heat is related to the exchange constants in a similar way.

NMR, spin-resonance, and specific-heat measurements at low temperatures are primarily sen-

sitive to the low-energy part of the spin-wave spectrum, which is considerably influenced by dipolar forces. Reasonable estimates of the dipolar contribution to the spin-wave energies can be made; nevertheless, integral measurements such as these often only accurately determine the spin-wave stiffness constant D, a particular linear combination of the exchange constants. By contrast, when inelastic neutron scattering is used to measure the *entire* spin-wave spectrum, not only the value of D but also the values of the nn and nnn exchange constants, J_1 and J_2, can be separately determined. All of these points will be discussed in more detail in Sec. VI.

III. EXPERIMENTAL METHOD

A. Spin-wave measurements with powder samples

As was noted above, difficulties with neutron absorption made it necessary to employ thin-slab samples. This in effect limited us to polycrystalline powders because thin single-crystal slabs of ^{153}EuO and ^{153}EuS of the required size were not available. With most magnetic materials, the direct measurement of spin-wave energies using powder samples would be impossible. Fortunately, isotropic ferromagnets are an exception to this rule. Let us consider why this is so.

As shown in Fig. 1, when neutrons of wave vector $\vec{k}_i$ are scattered to wave vector $\vec{k}_f$, energy and momentum conservation in the scattering process require that

$$\hbar\omega = (\hbar^2/2m)(k_i^2 - k_f^2) \tag{2}$$

and

$$\vec{\kappa} \equiv \vec{k}_i - \vec{k}_f = \vec{q} + \vec{\tau}. \tag{3}$$

In ferromagnets, spin-wave scattering occurs around *all* reciprocal-lattice vectors. This includes $\vec{\tau}(0, 0, 0)$, the only reciprocal-lattice vector which is well defined in a powder, the others being distributed uniformly over spheres surrounding the origin. Around $\vec{\tau}(0, 0, 0)$, $\vec{\kappa} = \vec{q}$. For small scattering angles, i.e., for small values of $\vec{q}$, the spin-wave exchange energies depend only on the modulus of $\vec{q}$ through the relation $\hbar\omega(\vec{q}) = Dq^2$. In high-symmetry lattices when both nn and nnn exchange are ferromagnetic, the spin-wave energies at larger values of q within the first Brillouin zone continue to depend only on the modulus of $\vec{q}$, i.e., the dispersion remains isotropic. In such cases the energy distribution of neutrons scattered around the forward direction in a powder will be identical to that observed in a single crystal at the same q. More commonly, however, the spin-wave energy at larger values of q varies markedly with the direction of propagation in a way determined by both the signs and magnitudes of J_1 and J_2 and the structure of the lattice.

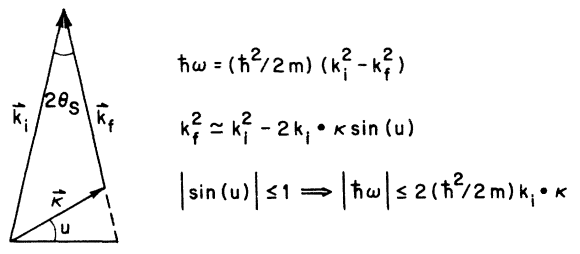

FIG. 1. Scattering diagram for inelastic scattering around the forward direction. Only excitations at energies (in meV) of less than $4.14k_i\kappa$ (Å^2) are accessible in inelastic scattering studies.

Fortunately, because the fcc lattice is highly symmetric, spin-wave dispersion in EuS is fairly isotropic; in EuO the combination of a fcc lattice and favorable values of J_1 and J_2 produce a remarkably isotropic dispersion. Powder broadening within the first Brillouin zone is consequently almost absent in EuO; in EuS it is more evident, but the spin-wave lines can still be identified without difficulty.

Obviously, powder broadening severely limits the possibilities for linewidth measurements. In addition, it makes identification of the energies of individual spin waves more difficult, but, as will be explained in Sec. IV, the exchange constants can still be determined from the data by appropriate analysis.

Aside from powder broadening, there are also several minor problems with small-angle-scattering measurements which ought to be mentioned. One is that the range of energy transfers available is much more restricted, as is evident in Fig. 1. This is not a problem in either EuO or EuS, where the spin-wave energies are small, but it can become important in other materials in which the energies are larger. A second difficulty is that the background at small angles contains an angularly dependent contribution from the primary beam. This can always be kept small by careful collimation and only becomes a serious problem at angles less than roughly 2°.

B. Neutron scattering measurements

All measurements were made near the forward direction in the constant-q mode with a triple-axis spectrometer using pyrolytic graphite monochromating and analyzing crystals. 13.5-meV neutrons were used for most measurements; however, for some of the smallest spin-wave energies 4.8-meV neutrons were employed. In every case filters

were placed in the beam incident on the sample to remove higher-order contamination.

C. Samples and thermometry

The samples were prepared[17] as fine polycrystalline powders of ^{153}EuO and ^{153}EuS and sealed in thin-walled aluminum holders in a helium atmosphere. The EuO sample weighed 0.745 g, was 24.1 mm high, 11.5 mm wide, and 0.50 mm thick; the EuS sample weighed 0.965 g, was 51.6 mm high, 12.0 mm wide, and 0.50 mm thick.

In each sample, the Curie temperature T_C was identified by finding the temperature corresponding to the peak of the critical scattering at the smallest possible wave vector, typically $q = 0.05$ Å^{-1}. In EuO we determined $T_C = 69.15 \pm 0.05$ K using a calibrated Pt resistance thermometer. In EuS we found $T_C = 16.57 \pm 0.02$ K using a Ge cryoresistor calibrated against a H_2-vapor thermometer. The observed values of T_C fall within the range reported in the literature for samples of good purity and stoichiometry. Neutron and x-ray powder diffraction patterns also showed no evidence of inclusions of other europium compounds in either sample. During the spin-wave measurements the samples were maintained at 5.5 °K.

IV. ANALYSIS OF THE DATA

In Figs. 2 and 3 the open circles represent the peak positions of the powder-broadened spin-wave lines as observed in EuO and EuS at various values of $|\vec{q}|$. To obtain from these observations the values of the exchange constants, we assumed that the spin-wave energies in the absence of an applied magnetic field are determined simply by exchange and dipolar interactions. Then, following Keffer[18] Eq. (14.9), we can use for the spin-wave energy, $\hbar\omega_{\vec{q}}$, the expression

$$\hbar\omega_{\vec{q}} = (A_{\vec{q}}^2 - |B_{\vec{q}}|^2)^{1/2}, \tag{4}$$

where, in our notation,

$$A_{\vec{q}} = 2S[J(0) - J(\vec{q})] + NS(g\mu_B)^2[\mathfrak{D}^{zz}(0) + \tfrac{1}{2}\mathfrak{D}^{zz}(q)],$$

$$B_{\vec{q}} = \tfrac{1}{2}SN(g\mu_B)^2[\mathfrak{D}^{xx}(\vec{q}) - \mathfrak{D}^{yy}(\vec{q}) - 2i\mathfrak{D}^{xy}(\vec{q})],$$

and

$$\mathfrak{D}^{IJ}(\vec{q}) = \frac{1}{N}\sum_{\vec{r}}{}'(3r^I r^J - r^2\delta^{IJ})r^{-5}e^{-i\vec{q}\cdot\vec{r}}.$$

The component indices I and J refer to a coordinate system with the z axis along the preferred spin direction. In EuO and EuS this is the ⟨111⟩ crystallographic direction. (See the discussion at the end of this section.)

If we include only nn and nnn exchange interactions, $J(\vec{q})$, which is by definition

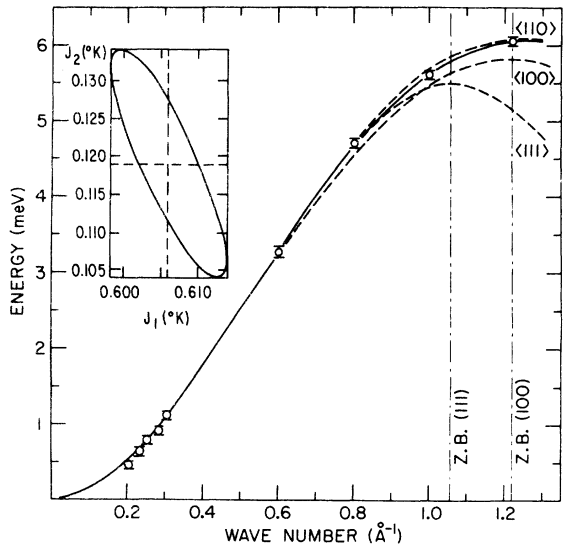

FIG. 2. Spin-wave dispersion in EuO powder at 5.5 K. The remarkable isotropy of the spin-wave dispersion is evident in the similarity of dispersion curves for spin waves propagating in the ⟨110⟩, ⟨100⟩, and ⟨111⟩ directions. The solid line represents the powder-averaged dispersion computed using the best-fitting values of J_1 and J_2, i.e., the central values of the covariance ellipse shown in the inset. The statistical probability that the true values of J_1 and J_2 are within the covariance ellipse is $1 - e^{-0.5} = 0.39$ and the probability that they are within the outer rectangle is 0.68.

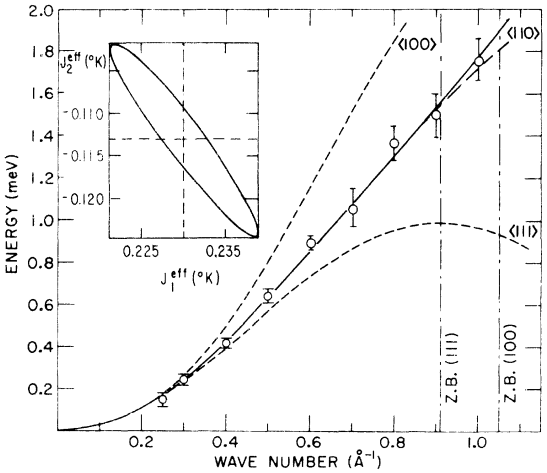

FIG. 3. Spin-wave dispersion in EuS powder at 5.5 K. Because J_2 is negative, spin-wave energies are quite different at larger values of q for different directions of propagation. The solid line represents the powder-averaged dispersion computed using the best-fitting values of J_1^{eff} and J_2^{eff}, i.e., the central values of the covariance ellipse shown in the inset. The exchange constants at 0 °K were deduced using Dyson's renormalization theory: they are $J_1 = 0.236 \pm 0.009$ K, $J_2 = -0.118 \pm 0.011$ K.

$$\sum_{\vec{r}} J(\vec{r}) e^{i\vec{q}\cdot\vec{r}},$$

reduces to

$$J_1 \sum_{\vec{r}_1} e^{i\vec{q}\cdot\vec{r}_1} + J_2 \sum_{\vec{r}_2} e^{i\vec{q}\cdot\vec{r}_2}.$$

The first term in $A_{\vec{q}}$, the exchange part, then takes the form

$$E_{ex}(\vec{q}) = 2S\left(12J_1 + 6J_2 - J_1 \sum_{\vec{r}_1} \cos(\vec{q}\cdot\vec{r}_1) - J_2 \sum_{\vec{r}_2} \cos(\vec{q}\cdot\vec{r}_1)\right).$$

For small $\vec{q}$, $E_{ex}(\vec{q})$ becomes isotropic and assumes the form Dq^2. The "stiffness constant" D is defined as $2Sa^2(J_1 + J_2)$ with a being the cube edge.

The other terms in $A_{\vec{q}}$ together with $B_{\vec{q}}$ are the dipolar contributions expressed as lattice sums. These $\vec{q}$-dependent sums can be evaluated easily in the region of q space where our neutron scattering data were obtained since the phase factors in the summations assure rapid convergence. But $\mathfrak{D}^{zz}(0)$, which appears in $A_{\vec{q}}$, constitutes a nontrivial problem because the convergence is so slow that the result depends on the summation boundary. It is customary to perform the summation over a sphere of arbitrary radius around the origin and replace the summation outside this sphere by an integral. In our case the summation over the inner sphere vanishes because of cubic symmetry. As for the volume integral outside the sphere, it can be transformed into a sum of two surface integrals, i.e., a surface integral over the sphere, conventionally called the Lorentz $\frac{4}{3}\pi$ factor, and a surface integral over the outer domain boundary, which is called the demagnetization factor N^z. Hence, in our case

$$\mathfrak{D}^{zz}(0) = \tfrac{4}{3}\pi - N^z.$$

If the domain happens to be spherical, $N^z = \frac{4}{3}\pi$ and $\mathfrak{D}^{zz}(0)$ vanishes. A spherical domain is very unlikely, however, since it means that a large amount of energy is stored in the magnetic field of the surface poles. This magnetic energy can be almost completely eliminated in zero external field if the system forms needle-shaped domains with adjacent domains oppositely oriented. In this case, $N^z = 0$. But the surface field energy is minimized in this configuration by breaking ferromagnetic exchange bonds. Obviously, the true domain shape must be something between a needle and a sphere, but we have no direct way of determining what it is in our powder samples. We assumed $N^z = 0$, an assumption that we will later show is consistent with our data. In this regard, it should be noted that in zero magnetic field a finite value of N^z will cause $A_{\vec{q}}$ to become negative for small $\vec{q}$ and the spin-wave theory would not be valid.

$\mathfrak{D}^{IJ}(\vec{q})$ can be expanded in $\vec{q}$ in the following way:

$$\mathfrak{D}^{IJ}(q) = \frac{4\pi}{3}\left(\delta^{IJ} - 3\frac{q^I q^J}{q^2} + O(q^2) + \cdots\right).$$

Retaining only the first two terms, the spin-wave energy for zero external field and $N^z = 0$ takes the form

$$\hbar\omega(\vec{q}) = E_{ex}(\vec{q})[1 + \phi(\vec{q})\sin^2\theta_{\vec{q}}]^{1/2}, \tag{5}$$

where

$$\phi(\vec{q}) = 4\pi N(g\mu_B)^2 S/E_{ex}(\vec{q}) = 4\pi g\mu_B M/E_{ex}(\vec{q})$$

and $\theta_{\vec{q}}$ is the angle between $\vec{q}$ and the direction of magnetization $\vec{M}$. We have compared this approximate expression with the results obtained by computing the full lattice sums (using the Ewald summation technique for rapid convergence) and have found that they agree to within two parts in 10^3 over the entire Brillouin zone. Hence, Eq. (5) was used to analyze our data.

All directions of $\vec{q}$ are equally probable in a powder. Therefore, as we have said, what we observe at a given $|\vec{q}|$ is a distribution of spin-wave energies, i.e., a "line shape" which can be computed by averaging Eq. (5) over all *directions* of $\vec{q}$ for assumed values of the exchange constants. To obtain the exchange constants the peak positions of the computed lines are least-squares fitted to the observed positions using J_1 and J_2 as variables of the fit. In Figs. 2 and 3 the solid lines represent the best-fitting "powder-averaged" dispersion curves using for J_1 and J_2 the central values of the covariance ellipses in the insets to the figures.

It should be noted that the spin-wave energies in the figures are those measured at a *finite* temperature, 5.5 K. In EuS this temperature is not negligible in comparison with T_C and the spin-wave energies are lower than their 0-K values. We used the spin-wave renormalization theory of Dyson[19] and of Keffer and Loudon[19] to extrapolate from the spin-wave energies observed at a finite temperature to the corresponding values at $T = 0$ K. In EuS the renormalization correction was 2.7% for J_1, 4.0% for J_2, and 7% for the magnetization entering $\phi(\vec{q})$ in Eq. (5). The correction was negligible in EuO. Since the theory agreed well with both our studies of spin-wave renormalization in EuO below T_C (discussed in paper III of this series) and with the observed decrease in magnetization with increasing temperature (discussed in paper II) we believe that the corrections to J_1 and J_2 are reliable and do not contribute to the uncertainty of these quantities.

We have used some of our spin-wave data at 30

K in EuO (paper III) to test the validity of Eq. (5). These data were obtained with high resolution (incoming neutron energy 4.8 meV) in the small-q region where $E_{ex}(\vec{q})$, the exchange part of the spin-wave energy, is well approximated by Dq^2. $E_{ex}(\vec{q})$ is therefore isotropic and Eq. (5) can be averaged analytically over all q directions to give

$$\langle \hbar\omega_q \rangle = Dq^2\left(\frac{1}{2} + \frac{1+\phi}{2\sqrt{\phi}} \arctan\sqrt{\phi}\right), \qquad (6)$$

where ϕ is defined by assuming in Eq. (5) that $E_{ex}(\vec{q}) = Dq^2$. Our calculations of renormalization in EuO have shown that at 30 K the magnetization is reduced by 10.8%, J_1 by 6.1%, and J_2 by 7.4%. Using for $4\pi M$ at $T = 0$ the value 24 kOe,[8] we obtain for D and ϕ in the above equations 10.8 meV Å^2 and 0.0248 q^{-2} Å^{-2}, respectively, at 30 K. In Fig. 4 the calculated and measured spin-wave energies are plotted versus q^2. The dipolar contribution appears as an almost constant amount added to the exchange energy Dq^2 which is shown as a dashed line in the figure. There is excellent agreement between calculated and measured energies indicating that the assumption of vanishing demagnetization factor N^z is consistent with the data. It is also an indication of the over-all reliability of the renormalization computation.

Referring again to Figs. 2 and 3, we have plotted the dispersion curves calculated along a few representative directions using the best-fitting exchange constants. It is evident that when J_1 and J_2 are of the same sign, as is the case in EuO, spin-wave dispersion is very isotropic and powder broadening is small. On the other hand, when the exchange constants are of opposite sign, as occurs in EuS, powder broadening increases.

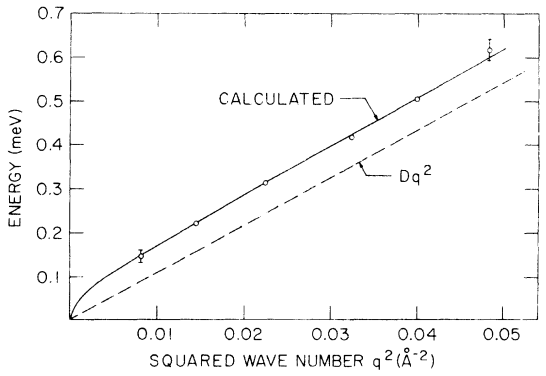

FIG. 4. Spin-wave energy vs q^2 at 30 K. The dashed line represents the exchange part Dq^2, with the stiffness constant D renormalized according to our calculations of dynamical interactions. The solid curve, which fits the measured energies exceedingly well, was calculated by including the dipolar contribution, assuming that the demagnetization factor $N^z = 0$.

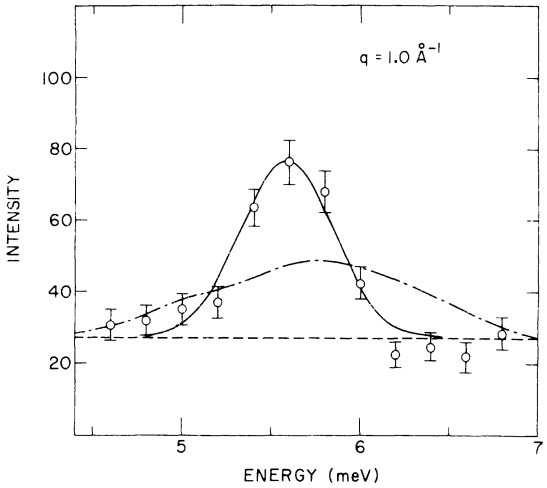

FIG. 5. Neutron line shape from scattering of spin waves of wave number 1.0 Å^{-1} in EuO powder. The solid line is the folding of the experimental resolution (width 0.6 meV) with the powder-broadened cross section (width 0.15 meV) for $J_1/k_B = 0.606$ K and $J_2/k_B = 0.119$ K. The dashed-dotted curve represents the same folding but using the values from Ref. 8, $J_1/k_B = 0.75$ K, $J_2/k_B = -0.098$ K (width 1.3 meV). The observed line profile clearly shows that the latter values for J_1 and J_2 cannot be correct.

Figure 5 shows the measured line profile in EuO close to the zone boundary. The solid curve represents the powder-broadened cross section folded with the experimental resolution. Since the resolution width (0.6 meV) is almost the same as the observed width of the neutron group, it is obvious that powder broadening cannot be larger than about 0.3 meV. Using the values of J_1 and J_2 from Fig. 2 we calculate the powder-broadened width to be 0.15 meV, consistent with the above. On the other hand, if we use the values for J_1 and J_2 reported in the specific-heat and NMR measurements[6,8] we obtain a powder-broadened width of 1.3 meV—completely incompatible with our observations.

It is perhaps also appropriate to comment in passing on several terms which we did not include in our data analysis. One is the effect of the spin-wave gap produced by crystalline electric fields. This can be estimated for both EuO and EuS by using the measured magnetic anisotropies.[20,21] The anisotropy energy E_a for a cubic crystal is given by

$$E_a = K_1(\alpha_1^2\alpha_2^2 + \alpha_2^2\alpha_3^2 + \alpha_3^2\alpha_1^2) + K_2\alpha_1^2\alpha_2^2\alpha_3^2,$$

where the α_i are direction cosines of the magnetization with respect to the cube edges. In both EuO and EuS the anisotropy constant K_1 is negative and $|K_1| \gg |K_2|$, hence the easy direction of magnetization is along any ⟨111⟩ axis. In EuO, $K_1 = -4.36 \times 10^5$ erg/cm^3 $= -0.009\,27$ meV per Eu ion. This

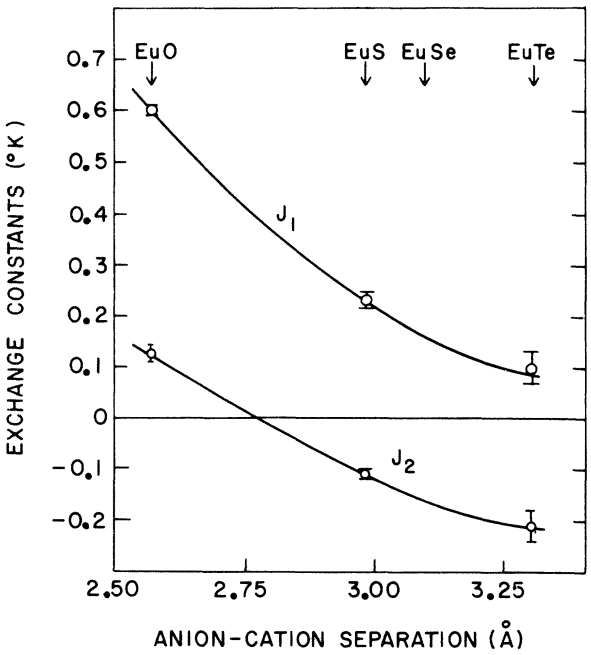

FIG. 6. Exchange constants in Eu chalcogenides versus anion-cation separation. The solid lines are simply smooth lines joining the points and have no theoretical significance.

number immediately indicates that the crystalline field hardly affects the spin-wave spectrum. Analysis[22] of the corresponding gap in the spin-wave dispersion gave a gap energy of $-(\frac{4}{3}K_1/S) = 0.00353$ meV. The anisotropy constant K_1 of EuS is an order of magnitude smaller than that of EuO, hence the effect of the crystalline field on the spin-wave dispersion of EuS can also be neglected.

Finally, we have not made allowances for zero-point motion nor have we included any Zeeman term in the Hamiltonian, such as for example that due to interdomain fields in magnetic powders. Our analysis indicated that such effects could not significantly influence the results.

V. RESULTS: COMPARISONS WITH THEORY

A. Comparison of exchange constants in the europium chalcogenides

Following McGuire and Shafer,[23] we have plotted in Fig. 6 our measured values for the exchange constants of EuO and EuS as a function of anion-cation separation together with the available values for other divalent chalcogenides. The regular variation with interionic distance is similar to that observed in the divalent samarium chalcogenides[24] and is consistent with Kasuya's[16] interpretation of the underlying exchange mechanisms.

Kasuya attempted to make a rough estimate of the value of J_1 for EuO. The result, 0.41 K, is in acceptable agreement with the measured value, 0.61 K, considering the highly approximate nature of the theory.

B. Relation of exchange constants to T_C

The critical temperature T_C is determined by the exchange constants and the dipolar forces. In the *mean-field* approximation one finds in fcc lattices[25]

$$T_C^{\mathrm{MF}} = \tfrac{2}{3}S(S+1)\sum_{\vec{r}} J(\vec{r})(1+g^{\mathrm{MF}}). \tag{7}$$

The second term represents the relative contribution to T_C, in the mean-field approximation, of the dipolar forces. In EuO, $g^{\mathrm{MF}} = 0.017$; in EuS, $g^{\mathrm{MF}} = 0.049$.[25]

More sophisticated theories employing series-expansion techniques have established that the mean-field approximation generally overestimates the critical temperature of the Heisenberg model. For nn interactions only, one finds that $T_C^{\mathrm{H}}/[\frac{2}{3}S(S+1)(12J_1)] = 0.790$ for the fcc Heisenberg model with $S = \frac{7}{2}$.[26] Wood and Dalton[27] have included nnn interactions and they find

$$T_C^{\mathrm{H}} = T_C^{\mathrm{H}}(J_2 = 0)[1 + 0.619(J_2/J_1)],$$

again for the fcc Heisenberg model with $S = \frac{7}{2}$. In generalizing Eq. (7) for the $S = \frac{7}{2}$ fcc lattice we set

$$T_C = 0.790[\tfrac{2}{3}S(S+1)(12J_1)] \times [1 + 0.619(J_2/J_1)](1+\hat{g}), \tag{8}$$

with $\hat{g}$ representing the contribution from dipolar forces. At the moment there are no better estimates of $\hat{g}$ than that obtained from the mean-field approximation. According to Fisher[28] $\hat{g}$ could vary from possibly $\frac{1}{5}\hat{g}^{\mathrm{MF}}$ to $5\hat{g}^{\mathrm{MF}}$ and might even have the opposite sign to $\hat{g}^{\mathrm{MF}}$.

In Fig. 7 we show the relation between J_1 and J_2 imposed by Eq. (8) with $\hat{g} = 0$ for $T_C = 16.57$ K and $T_C = 69.15$ K. Our neutron scattering results are also included as covariance ellipses taken from Figs. 2 and 3. The agreement between experiment and theory, which has also been remarked by Collins,[29] is most satisfactory and gives additional support to the view that EuO and EuS are indeed simple Heisenberg ferromagnets.

VI. RESULTS: COMPARISON WITH OTHER MEASUREMENTS

A. NMR, specific heat, and spin resonance

We mentioned briefly in Sec. II that information about exchange constants in EuO and EuS has also been obtained from low-temperature specific-heat[5,6] and NMR[7,8] measurements and from rf excitation of standing spin waves in thin films.[11] The results of these measurements are summarized

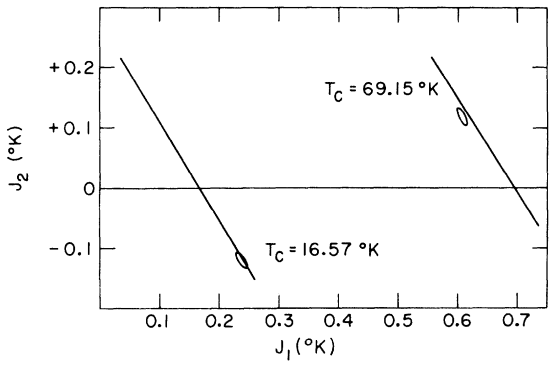

FIG. 7. Critical temperature T_C depends on the exchange constants J_1 and J_2. The solid lines represent the correlation between J_1 and J_2 with, respectively, $T_C = 16.57$ K and $T_C = 69.15$ K required by series expansions for the Heisenberg model (Ref. 27). The neutron scattering results for (J_1, J_2) are taken from Figs. 2 and 3.

in Table I. For EuS there is a fair degree of consistency except for the spin-wave resonance measurements, but for EuO there are obvious discrepancies. Let us therefore examine each method in more detail to see if we can understand how experiments, which agree reasonably well in one case can disagree in what is apparently an almost identical situation.[30]

NMR measurements are, in effect, a determination of the variation of the magnetization with temperature. Each time a spin wave is thermally excited the magnetization drops by $g\mu_B$, hence, the relative change in the magnetization $\Delta M/M_0$ for a system of N spins is

$$(NS)^{-1}\sum_{\vec{q}}\langle n_{\vec{q}}\rangle ,$$

where $\langle n_{\vec{q}}\rangle$ is the Bose distribution function $\{\exp[h\omega(\vec{q})/k_BT]-1\}^{-1}$. The specific heat per magnetic ion C is the temperature derivative of the magnetic energy per ion, i.e., the derivative of

$$N^{-1}\sum_{\vec{q}} h\omega(\vec{q})\langle n_{\vec{q}}\rangle .$$

It is customary to replace the summation over all $\vec{q}$ vectors in the Brillouin zone by an integration over $|\vec{q}|$, thus obtaining the approximate expressions

$$\frac{\Delta M}{M_0}\alpha\int q^2\langle n_{\vec{q}}\rangle dq$$

and

$$C\propto\int q^2 h\omega(q)\frac{\partial}{\partial T}\langle n_{\vec{q}}\rangle dq .$$

In Fig. 8 the integrands of the above expressions are plotted for EuO at 2 and 4 K, temperatures appropriate to the NMR and specific-heat experiments. To calculate $\Delta M/M_0$ and C we performed an exact summation over the Brillouin zone using the same approximations for the dipolar energy as were used to the analyses of the NMR and specific-heat measurements [Eq. (14) of Ref. 7, which is identical to our Eq. (5)]. It is evident from the figure that in EuO these experiments sample the low-energy part of the spin-wave spectrum where the exchange energy is only dependent on the stiffness constant D. In this case the individual values of J_1 and J_2 cannot be determined by either technique. This is very evident in Fig. 9 which shows the covariance ellipse for J_1 and J_2 for EuO resulting from our reanalysis of the specific-heat data of Ref. 6 (following Ref. 6 the demagnetization field H in our analysis was set equal to zero). It is seen that the covariance ellipse simply degenerates into a parallel band of slope -1, indicating that only the sum J_1+J_2 is determined. For reference, the neutron scattering results are also shown as the covariance ellipse taken from Fig. 2. It is clear that the specific-heat and neutron scattering measurements yield essentially the same value of the spin-wave stiffness constant D. We

TABLE I. Exchange constants in K. [a]

	EuO			EuS		
	J_1	J_2	J_1+J_2	J_1	J_2	J_1+J_2
This expt.	0.606 ± 0.008	0.119 ± 0.015	0.725 ± 0.006	0.236 ± 0.009	−0.118 ± 0.011	0.118 ± 0.006
Specific heat quoted values	0.76 ± 0.02 [b]	−0.084 ± 0.015 [b]	0.68 ± 0.03	0.20 [c]	−0.06 [c]	0.14 ± 0.02 [c,d]
Specific heat reanalyzed	undetermined		0.714 ± 0.007	0.228 ± 0.003	−0.102 ± 0.005	0.126 ± 0.004
NMR	0.75 ± 0.0025 [e]	−0.0975 ± 0.004 [e]	0.653 ± 0.005	0.20 ± 0.01 [f]	−0.08 ± 0.02 [f]	0.12 ± 0.02
Spin resonance						0.088 ± 0.010 [d]

[a] Exchange constants as defined in Eq. (1).
[b] Reference 6.
[c] Reference 5.
[d] Reference 11.
[e] Reference 8.
[f] Reference 7.

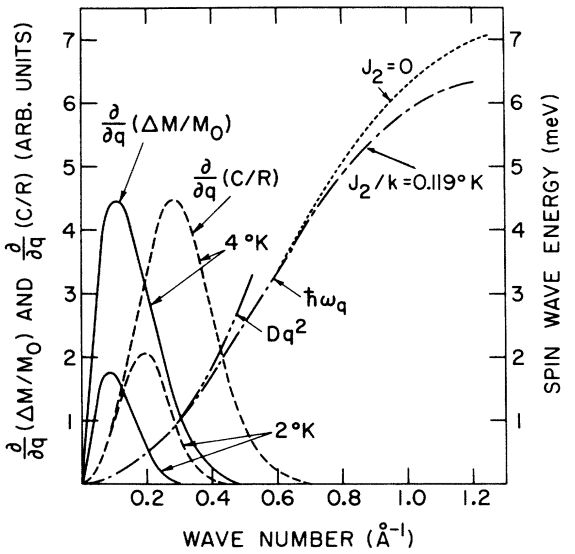

FIG. 8. Sensitivity of NMR and specific-heat measurements to J_1 and J_2. The dash-dotted curve represents spin-wave dispersion in the ⟨110⟩ direction for EuO using our best values of J_1 and J_2 and including dipolar contributions. The dotted curve has the same stiffness constant D but $J_2=0$. It is evident that the individual values of J_1 and J_2 are important only within the second half of the Brillouin zone. The solid curves represent the calculated contribution from different q shells in the Brillouin zone to the decrease in magnetization at 2 and 4 K as measured by NMR. Likewise, the dashed curves are the differential contributions to the specific heat. Both techniques applied below 4 K only sample the first half of the Brillouin zone and therefore only determine J_1+J_2. In addition, the NMR measurements are particularly dependent on a good estimate of the dipolar energy.

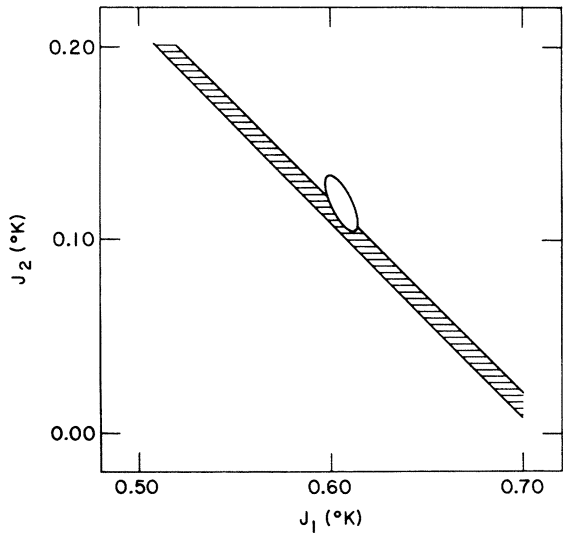

FIG. 9. Covariance "ellipse" for J_1 and J_2 in EuO from our reanalysis of the specific-heat measurements of Henderson, Brown, Reed, and Meyer (Ref. 6). The covariance ellipse has degenerated into a paralled band of slope -1 showing that only J_1+J_2 is determined. The corresponding ellipse from neutron scattering (taken from Fig. 2) is shown for reference.

cannot explain, however, why the authors of Ref. 6 obtained $J_1/k_B=-0.76$ °K and $J_2/k_B=-0.084$ °K, values significantly outside the covariance band we calculated using the same method of analysis.

The NMR measurements are extremely dependent on good estimates of the dipolar energy and are therefore less accurate than either the specific-heat or neutron scattering measurements. Reanalysis of the NMR data for EuO shows that in order to obtain a satisfactory fit, whatever the values of J_1+J_2, it is necessary to introduce an energy gap [through the field H in Eq. (14) of Ref. 7]. The observed magnetization is well represented by using our value of the stiffness constant and an internal field of 2.4 kOe, corresponding to an energy gap of 0.03 meV. Whether this small gap is real is difficult to say. While it has no effect on the neutron scattering results, it cannot easily be reconciled with the specific-heat analysis.

In EuS the situation is different, because the spin-wave energies are smaller than in EuO. At 4.2 °K, the outer half of the Brillouin zone contributes about $\frac{2}{3}$ of the specific heat in contrast to EuO where this contribution is negligibly small. Thus in EuS the specific heat C between 1 and 4 K depends on the entire dispersion curve, although the NMR measurements[7] in the same temperature region are still confined to the low-q region of the Brillouin zone.

We have reanalyzed the specific-heat data of Passenheim *et al.*[5] and found that we could obtain an excellent fit to their measurements both for zero internal field and for $H_{\text{int}}=5.82$ and 10.8 kOe. Their data are reproduced in Fig. 10 along with our best fits for $J_1=0.228$ and $J_2=-0.102$ K. The inset shows the covariance ellipses for both specific-heat and neutron scattering measurements (taken from Fig. 3). To calculate the covariance ellipse for the specific-heat data we assumed an uncertainty in C of the size of the solid circles in Fig. 10. Since we believe this is a conservative estimate, the covariance ellipse for C might actually be smaller than that shown in the figure. Keeping in mind that covariance ellipses represent 39% probability limits, it is evident that the agreement between neutron scattering and specific-heat results is satisfactory. In fact, the specific-heat measurements appear in this case to provide a better determination of J_1 and J_2 than the neutron scattering measurements because the anisotropy in the spin-wave dispersion reduces the sensitivity of the latter.

We believe that our reanalysis of the measure-

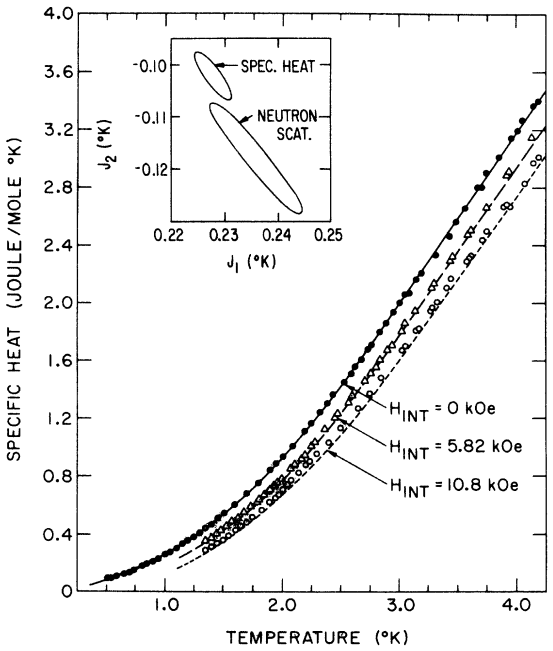

FIG. 10. Magnetic specific heat of EuS. The points are measurements by Passenheim, McCollum, and Callaway (Ref. 5) for three internal magnetic fields. The curves are our calculations using exact Brillouin-zone sums. The covariance ellipse for J_1 and J_2 from the best fit at $H_{int}=0$ is shown in the inset together with the corresponding covariance ellipse from our neutron scattering measurements (taken from Fig. 3).

ments of Passenheim *et al.*[5] gives better values for J_1 and J_2 in EuS than those originally quoted. The reason is that while the same approximation for the dipolar energy [Eq. (14) of Ref. 7], was used, we also took into account the renormalization of the spin-wave energies. Although this had a significant effect, we should mention that it does not entirely account for the differences between our values of the exchange constants and those obtained in the original analysis. Therefore, we also suspect that there is a computational error in Ref. 5, possibly in the Brillouin-zone sums.

B. Pressure dependence of T_C

According to Fig. 6, both J_1 and J_2 vary in a smooth and regular way as the interionic distance changes. We mentioned earlier that this also occurs in the Sm chalcogenides,[24] and it is tempting to interpret it as indicating that replacing one anion by another is simply equivalent to expanding or contracting the lattice. The concept can be tested by taking values of dJ_1/da and dJ_2/da from Fig. 6 and checking to see if these values are consistent with the measured variation of T_C with atomic volume, i.e., with the measured variation of $d(\ln T_C)/d(\ln V)$. The expected relationship between the two quantities is easily derived by differentiating Eq. (7) which yields

$$\frac{\Delta T_C}{T_C} = \frac{dJ_1/da + \frac{1}{2}(dJ_2/da)}{J_1 + \frac{1}{2}J_2}\,\Delta a\,,$$

from which it follows that

$$\frac{d(\ln T_C)}{d(\ln V)} = \frac{\Delta T_C/T_C}{3\Delta a/a} = \frac{a}{3}\left[\frac{dJ_1/da + \frac{1}{2}(dJ_2/da)}{J_1 + J_2}\right]. \quad (9)$$

From the solid lines drawn through the points of Fig. 6 we find $dJ_1/da = -1.08$ K/Å and $dJ_2/da = -0.68$ K/Å for EuO and $dJ_1/da = -0.66$ K/Å and $dJ_2/da = -0.45$ K/Å for EuS, i.e., at $a = 2.57$ and 2.98 Å, respectively. Substituting these values in Eq. (9) yields for $d(\ln T_C)/d(\ln V)$ the value -2 for EuO and -5 for EuS. By comparison, from direct measurements of the pressure dependence of T_C one obtains for $d(\ln T_C)/d(\ln V)$ the value -6 ± 2 for EuO,[31-33] and -9 for EuS.[34]

Obviously the two sets of measurements are not consistent in either case. McWhan, Souers, and Jura,[32] noting essentially the same discrepancy, have suggested that it reflects changes in covalency in going from one anion to another. Possibly changes in covalency with pressure may also be involved.

VII. SUMMARY

We have shown that the exchange constants of EuO and EuS can be accurately determined by small-angle neutron scattering measurements on polycrystalline powders enriched in ^{153}Eu. Combining our data with results for EuTe we find that the exchange couplings of the Eu^{2+} ions vary in a smooth and regular way as the interionic distance changes. nn exchange is ferromagnetic at the largest distances (EuTe) and increases as the interionic distance decreases. nnn exchange is antiferromagnetic at the largest distances; it decreases as the interionic distance decreases and finally, according to our measurements (and in contradiction to earlier results), becomes ferromagnetic at small distances (EuO). This behavior is in accord with Kasuya's description of the underlying exchange mechanisms.

We find that series-expansion calculations of the ordering temperatures of EuO and EuS are consistent with the signs and magnitudes of the exchange constants as presently determined. Also the transition from antiferromagnetism in EuTe to two component antiferromagnetism and ferrimagnetism in EuSe and thence to ferromagnetism in EuS and EuO correlates well with the known behavior of the exchange interactions.

Finally, we note that our results are not consis-

tent with the idea that replacing one anion by another in the chalcogenide series is equivalent to simply expanding or contracting the lattice. The reasons for this are obscure but probably reflect the influence of anion covalency on the exchange interactions in these materials.

ACKNOWLEDGMENT

We wish to express our appreciation to Dr. W. Kunnmann for preparing the samples of ^{153}EuO and ^{153}EuS.

---

*Research sponsored by the U. S. Energy Research and Development Administration.

†Part of the work done while Guest Scientists at Brookhaven National Laboratory.

[1]B. T. Matthias, R. M. Bozorth, and J. H. Van Vleck, Phys. Rev. Lett. 7, 160 (1961).

[2]T. R. McGuire, B. E. Argyle, M. W. Shafer, and J. S. Smart, Appl. Phys. Lett. 1, 17 (1962).

[3]H. W. White, D. C. McCollum, and J. Callaway, Phys. Lett. A 25, 388 (1967). H. W. White, Ph.D. thesis (University of California, Riverside, 1969) (unpublished).

[4]G. Will, S. J. Pickart, H. A. Alperin, and R. Nathans, J. Phys. Chem. Solids 24, 1679 (1963).

[5]B. C. Passenheim, D. C. McCollum, and J. Callaway, Phys. Lett. 23, 634 (1966).

[6]A. J. Henderson, Jr., G. R. Brown, T. B. Reed, and H. Meyer, J. Appl. Phys. 41, 946 (1970).

[7]S. H. Charap and E. L. Boyd, Phys. Rev. 133, A811 (1964).

[8]E. L. Boyd, Phys. Rev. 145, 174 (1966).

[9]P. Heller and G. Benedek, Phys. Rev. Lett. 14, 71 (1965).

[10]N. Menyuk, K. Dwight, and T. B. Reed, Phys. Rev. B 3, 1689 (1971).

[11]P. K. Schwob and G. E. Everett, J. Phys. (Paris) Suppl. 32, 1066 (1971).

[12]J. Hog and T. Johansson, Int. J. Magn. 4, 11 (1973).

[13]J. Als-Nielsen, O. W. Dietrich, W. Kunnmann, and L. Passell, Phys. Rev. Lett. 27, 741 (1971).

[14]L. Passell, O. W. Dietrich, and J. Als-Nielsen, AIP Conf. Proc. 5, 1251 (1971).

[15]L. Passell, J. Als-Nielsen, and O. W. Dietrich, *Neutron Inelastic Scattering* (International Atomic Energy Agency, Vienna, 1972), p. 619.

[16]T. Kasuya, IBM J. Res. Dev. 14, 214 (1970).

[17]The samples used for these measurements were prepared by Dr. W. Kunnmann. For EuS he employed Archer and Mitchell's method [R. D. Archer and W. N. Mitchell, Inorg. Synth. X, 77 (1967)]. To remove the last traces of excess sulfur, the sample was heated to 1200 °C under a high rate of flow of oxygen and water-free hydrogen. Chemical analysis of the final product indicated the molar sulfur to europium ratio was 1.001 ± 0.001. EuO was prepared from Eu_2O_3 in powder form. Equal amounts were placed in the top and bottom sections of a tungsten crucible 0.5 cm in diameter and 7.5 cm long. A length of tungsten foil was inserted as a baffle separating the two sections. In the bottom section yttrium metal was added to the charge in the amount of $\frac{1}{3}$ the weight of the Eu_2O_3 in that section. The crucible was mounted in an argon-filled tube in an induction furnace in which the top section was heated to 1200 °C and the bottom section to 1800 °C. The yttrium metal in the hotter bottom section reacted with the Eu_2O_3 to form Eu vapor, which diffused into the top chamber and reacted to form a mixture of EuO and Eu metal. Excess metal was removed in a separate operation by vacuum sublimation at 800–1000 °C. Chemical analysis indicated a stoichiometric compound. Fluorescence tests for yttrium contamination were negative.

[18]F. Keffer, in *Encyclopedia of Physics* (Springer-Verlag, Berlin, 1966), Vol. XVIII/2, p. 1.

[19]F. J. Dyson, Phys. Rev. 102, 1217 (1956); 102, 1230 (1956); F. Keffer and R. Loudon, J. App. Phys. Suppl. 32, 25 (1961).

[20]N. Miyata and B. E. Argyle, Phys. Rev. 157, 448 (1967).

[21]M. C. Franzblau, G. E. Everett, and A. W. Laws, Phys. Rev. 164, 716 (1967).

[22]We are grateful to P. A. Lindgård for deriving the relation between the gap energy and the macroscopic anisotropy parameter K_1.

[23]T. R. McGuire and M. W. Shafer, J. Appl. Phys. 35, 984 (1964).

[24]R. J. Birgeneau, E. Bucher, L. W. Rupp, Jr., and W. M. Walsh, Jr., Phys. Rev. B 5, 3412 (1972).

[25]M. E. Fisher and A. Aharony, Phys. Rev. Lett. 30, 559 (1973).

[26]D. S. Ritchie and M. E. Fisher, Phys. Rev. B 5, 2668 (1972).

[27]D. W. Wood and N. W. Dalton, Phys. Rev. 159, 384 (1967).

[28]M. E. Fisher (private communication). We are grateful to Professor Fisher for discussing the influence of dipolar forces on T_C.

[29]M. F. Collins, J. Phys. C 7, 573 (1974).

[30]As a result of our neutron scattering studies the heat-capacity measurements of Refs. 5 and 6 and the NMR magnetization measurements of Refs. 7 and 8 have recently been reexamined. The results are reported by O. W. Dietrich, A. J. Henderson, Jr., and H. Meyer [Phys. Rev. B 12, 2844 (1975)].

[31]G. K. Sokolova, K. M. Demchuck, K. P. Rodionov, and A. A. Samokhvalov, Zh. Eksp. Teor. Fiz. 49, 452 (1965) [Sov. Phys.-JETP 22, 317 (1966)].

[32]D. B. McWhan, P. C. Souers, and G. Jura, Phys. Rev. 143, 385 (1966).

[33]K. Lee and J. C. Suits, J. Appl. Phys. 41, 954 (1970).

[34]Y. Hidaka, J. Sci. Hiroshima Univ. A 35, 93 (1971).